Wood-Fiber-Reinforced Poly(lactic acid) Composites: Evaluation of the Physicomechanical and Morphological Properties

M. S. Huda,[1] L. T. Drzal,[1] M. Misra,[1] A. K. Mohanty[2]

[1]*Composite Materials and Structures Center, 2100 Engineering Building, Michigan State University, East Lansing, Michigan 48824*
[2]*School of Packaging, 130 Packaging Building, Michigan State University, East Lansing, Michigan 48824*

Received 28 September 2005; accepted 26 April 2006
DOI 10.1002/app.24829
Published online in Wiley InterScience (www.interscience.wiley.com).

ABSTRACT: This article presents the results of a study of the processing and physicomechanical properties of environmentally friendly wood-fiber-reinforced poly(lactic acid) composites that were produced with a microcompounding molding system. Wood-fiber-reinforced polypropylene composites were also processed under similar conditions and were compared to wood-fiber-reinforced poly(lactic acid) composites. The mechanical, thermomechanical, and morphological properties of these composites were studied. In terms of the mechanical properties, the wood-fiber-reinforced poly(lactic acid) composites were comparable to conventional polypropylene-based thermoplastic composites. The mechanical properties of the wood-fiber-reinforced poly(lactic acid) composites were significantly higher than those of the virgin resin. The flexural modulus (8.9 GPa) of the wood-fiber-reinforced poly(lactic acid) composite (30 wt % fiber) was comparable to that of traditional (i.e., wood-fiber-reinforced polypropylene) composites (3.4 GPa). The incorporation of the wood fibers into poly(lactic acid) resulted in a considerable increase in the storage modulus (stiffness) of the resin. The addition of the maleated polypropylene coupling agent improved the mechanical properties of the composites. Microstructure studies using scanning electron microscopy indicated significant interfacial bonding between the matrix and the wood fibers. The specific performance evidenced by the wood-fiber-reinforced poly(lactic acid) composites may hint at potential applications in, for example, the automotive and packaging industries. © 2006 Wiley Periodicals, Inc. J Appl Polym Sci 102: 4856–4869, 2006

Key words: biodegradable; biofibers; biopolymers; renewable resources; thermal properties

INTRODUCTION

Plastic composites reinforced with wood fibers (WFs) are a group of new materials made from a combination of WFs and thermoplastic resins.[1] WF-reinforced composites are becoming increasingly popular in the furniture, automotive, and building industries.[1–3] However, thermoplastic users are still seeking new ways to improve product performance. In addition to the processing and physical properties, the long-term behavior of these materials is a very important parameter, especially with respect to the design layout and the product liability.[3–7] Moreover, the recent expansion in applications of WF-reinforced plastic composites brings requirements for a more uniform and accurate evaluation of product properties across the industry.

Although, when combined with thermoplastic polymers, WFs produce composite materials that are lightweight and recyclable and often possess high strength-to-weight ratios, the combination of WFs and thermoplastic polymers presents a number of problems.[1–3,5,6] In many instances, incompatibility between the fiber and matrix results in an inferior interface that does not adequately transfer stress to the load-bearing fiber. The structure–property relationships of several reinforcing natural fibers with biodegradable polymers have been recently analyzed,[7–11] and generally, the performance of these biomaterials is greatly influenced by both the properties of the fiber and the quality of the fiber/polymer-matrix adhesion. Several studies have been carried out to achieve high-performance, natural-fiber-reinforced thermoplastics through improvements in the compatibility between hydrophobic thermoplastics and hydrophilic cellulosic fibers.[9–11] In those studies, biocomposites, with pineapple leaf fibers, abaca, sisal, and so forth used as cellulosic natural fibers, were examined to improve the low mechani-

Correspondence to: M. Misra (misraman@egr.msu.edu).
Contract grant sponsor: National Science Foundation; contract grant numbers: DMI-0400296 (for the project ''PREMISE-II: Design and Engineering of 'Green' Composites from Biofibers and Bioplastics''), DMR-0216865 (through the Instrumentation for Materials Research program).
Contract grant sponsor: U.S. Department of Agriculture-MB International; contract grant number: 2002-34189-12748-S4057 (for the project ''Bioprocessing for Utilization of Agricultural Resources'').

cal properties. The further development of applications of renewable biofibers (e.g., WFs) in the plastic industry could provide attractive, new value-added markets for agricultural products while simultaneously displacing petrochemical-based plastic resins.

One of the most promising biodegradable polymers is poly(lactic acid) (PLA), which can be derived from renewable resources, such as corn.[12] Composites containing biodegradable polymers, such as PLA, and WFs offer an interesting combination of properties as well as lower cost than competitive materials. PLA is a linear, aliphatic, thermoplastic polyester produced from a lactic acid byproduct obtained from the fermentation of corn dextrose.[12] The Nebraska facility of Cargill Dow is capable of producing up to 300 million pounds (140,000 metric tons) of PLA per year, using 40,000 bushels of corn per day,[13] and production is expected to more than triple to 1 billion pounds by 2007.[14] PLA is well known for its highly biocompatible and biodegradable nature[12] and has received considerable industrial attention for use in commodity resins capable of replacing petrochemical-based polymers. PLA has better mechanical properties than polypropylene (PP). Pure PLA has a tensile strength of 62 MPa and a modulus of 2.7 GPa, in contrast to 36 MPa and 1.2 GPa for pure PP.[15] Moreover, PLA can be processed by injection molding, blow molding, and film forming because the glass-transition temperature (T_g) of PLA is 54°C and the melting temperature (T_m) is 172°C.[15,16] Oksman et al.[16] showed that PLA–flax composites had better mechanical properties than PP–flax composites. Although PLA has mechanical properties suited for industrial plastic applications,[13,16] it is considered too brittle for many commercial applications. It is, however, possible to overcome the brittleness and poor processability of stiff and hard polymers through their combination with other materials. Most research on PLA composites ultimately seeks to improve the mechanical properties to a level that satisfies a particular application.[7,13] Some researchers consider the enhanced toughness the main advantage of biofibers in composites.[5,7,16] Because both components of the composite, the biopolymer (e.g., PLA) and biofiber (e.g., WF), are biodegradable, the composite as an integral part is also expected to be biodegradable.[8,17,18] Hence, because PLA can open many new opportunities in industrial bioplastic applications, there is a need to better understand and describe its properties as the matrix material for biocomposite materials.

A review of the literature shows that comparative studies of the thermal and mechanical properties of PLA-based composites containing different amounts of WFs are very limited. Therefore, the objectives of this study were to evaluate the mechanical and thermomechanical properties of WF-reinforced PLA composite materials that were processed with a microcompounding molding system. WF-reinforced PP composites were also processed with the microcompounding molding system and compared to PLA/WF composites. Because coupling agents help overcome the polarity disparity to increase the composite strength, maleated polypropylene (MAPP) was also used in this study. Generally, interactions between the hydroxyl groups of WFs and the anhydride groups of maleated coupling agents can overcome the incompatibility problem to increase the mechanical properties of WF-reinforced thermoplastic composites.[19] Kazayawoko and Balatinecz[5] suggested that coupling agents create a crosslinking structure on wood surfaces and some polymers, which is grafted onto wood by coupling agents; as a result, modified wood has a surface similar to the matrix. Additionally, coupling agents with a structure similar to the matrix are grafted onto wood, and this helps to improve interfacial adhesion. Carlson et al.[20] investigated the production of maleated polylactide by reactive extrusion. These authors demonstrated that improved interfacial adhesion could be obtained in PLA/starch blends through the modification of PLA with low levels of maleic anhydride (MA). The use of MA or MAPP in cellulose-reinforced thermoplastic composites has been reported by several scientists[21–24] assuming esterification between the solid cellulose and the anhydride moiety. Oksman et al.[25] used Fourier transform infrared (FTIR) spectroscopy to show that MA was partially bonded to the wood through esterification. Their results also indicated hydrogen bonds between hydroxyl groups on the wood surfaces and MA.[25] Although the interaction between the MA groups of MAPP with OH groups of WFs is very well established, the MA groups of MAPP might react with the terminal OH groups of PLA to create new linkages.[26,27] Because both PLA and PP have a hydrophobic nature,[12,24] the interaction between PLA and PP may not be established in this study. In addition, the amount of PP that is used in the composites as MAPP is much less in comparison with the PLA matrix. The best choice is the use of maleated PLA, which we have a plan to synthesize and use in our future studies. Kazayawoko et al.[23] and Lee et al.[26] suggested that by radical grafting, the double bond of MA could be reacted with methyl and methine carbons of PLA. Because of esterification and hydrogen bonding with hydroxyl groups on the WF surface, these grafted polymers could be effective as compatibilizers between the WF filler and polymer-matrix in a composite. The objectives of using MAPP as a coupling agent in this study were (1) to investigate the effects of the coupling agent on the mechanical properties of the resultant composites, (2) to investigate the influences of the compounding conditions on the

mechanical properties of the resultant composites, (3) to observe the interfacial morphology of the fracture surface and also the distribution of the coupling agent, (4) to examine the interfacial similarity rule with the WF–MAPP–PLA structure as well as the WF–MAPP–PP structure, and (5) to examine the effects of MAPP (e.g., Epolene G-3015 polymer) for the PP–WF interface in terms of the coupling performance. In this work, a PLA/MAPP (95/5 wt %) blend was prepared with a microcompounding molding system. In addition, the WF-reinforced PLA composites a composition of 65 wt % PLA/30 wt % WF/5 wt % MAPP. PP/MAPP (95 wt %/5 wt %) and PP/WF/MAPP (65 wt %/30 wt %/5 wt %) were also extruded under identical conditions, and the mechanical and thermomechanical properties were compared with those of the PLA-based composites.

EXPERIMENTAL

Materials

PLA (Biomer L 9000; weight-average molecular weight = 220 kDa, number-average molecular weight = 101 kDa) was obtained from Biomer (Krailling, Germany). WFs (2010 maple wood flour) was supplied by American Wood Fibers (Schofield, WI). PP (ProFax 6523) was obtained from Basell Polyolefins (Elkton, MD). MAPP (Epolene G-3015 polymer) was supplied by Eastman Chemical Co. (Kingsport, TN).

Fabrication of the composites with a microcompounding system

Before the processing, the WFs and PLA were dried *in vacuo* at 80°C for 24 h. The PP matrix, however, was not dried. The required amounts of the fibers and the polymer were mechanically mixed in a kitchen mixer (model 56200, type B17, Hamilton Beach, Washington, NC). Then, the samples were extruded at 100 rpm with a Micro 15-cc compounding system (DSM Research, Geleen, The Netherlands) at 183°C for 10 min.[28] The extruder had a screw length of 150 mm, a length/diameter ratio of 18, and a net capacity of 15 cm^3. To obtain the desired specimen samples for various measurements and analyses, the molten composite samples were transferred after extrusion through a preheated cylinder to a mini-injection molder, which was preset with an injection temperature at 183°C and a mold temperature at 40°C. Injection-molded samples were placed in sealed polyethylene bags to prevent moisture absorption.

Measurements

Mechanical testing

A mechanical testing machine (SFM 20, United Calibration Corp.) was used to measure the flexural properties according to ASTM Standard D 790 and the tensile properties according to ASTM Standard D 638. System control and data analysis were preformed with Datum software. The notched Izod impact strength was measured with a 43-02-01 monitor/impact machine from Testing Machines, Inc. (Syracuse, NY), according to ASTM D 256. All presented results are the average values of five measurements.

Dynamic mechanical analysis (DMA)

The storage modulus, loss modulus, and loss factor (tan δ) of the composite specimens were measured as a function of temperature (from 20 to 100°C for PLA-based composites and from −50 to 150°C for PP-based composites) with a TA 2980 dynamic mechanical analyzer (New Castle, DE) equipped with a dual-cantilever bending fixture at a frequency of 1 Hz and a heating constant rate of 5°C/min.

Heat defection temperature (HDT)

HDT measurements were obtained on injection-molded flexural bars at a 66 psi load according to ASTM Standard D 648 deflection test with a TA 2980 dynamic mechanical analyzer equipped with a dual-cantilever bending fixture at a heating rate of 2°C/min.

Thermogravimetric analysis (TGA)

TGA was carried out with a TA 2950 thermogravimetric analyzer (New Castle, DE). The samples were scanned from 25 to 600°C at 20°C/min in the presence of nitrogen.

Scanning electron microscopy (SEM)

The morphology of the impact fracture surfaces of the composites was observed with SEM at room temperature. A JEOL model JSM-6300F (Peabody, MA) scanning electron microscope with a field emission gun and accelerating voltage of 10 kV was used to collect SEM images for the composite specimens. A gold coating was placed on the impact fracture surfaces, and the samples were viewed perpendicularly to the fractured surface.

RESULTS AND DISCUSSION

Mechanical properties

Flexural properties of the composites

The flexural properties of the WF-reinforced PLA composites are given in Table I. The fiber content was varied from 20 to 40% to evaluate the effect of the loading on the mechanical properties. There is an appreciable

TABLE I
Flexural Properties of the Composites

Polymer/ fibers (wt %)	Flexural strength (MPa)	Flexural modulus (GPa)	Improvement in the modulus (%)
Neat PLA	98.8 ± 1.0	3.3 ± 0.1	—
PLA/WF (80/20)	118.3 ± 2.1	7.1 ± 0.2	115
PLA/WF (70/30)	116.6 ± 2.4	8.9 ± 0.8	169
PLA/WF (60/40)	114.3 ± 5.6	10.2 ± 0.9	209
Neat PP	32.9 ± 1.8	1.5 ± 0.2	—
PP/WF (80/20)	43.0 ± 1.2	2.7 ± 0.1	80
PP/WF (70/30)	51.4 ± 4.3	3.4 ± 0.9	126
PP/WF (60/40)	55.1 ± 2.4	4.6 ± 0.3	206

rise in the flexural strength at 20, 30, and 40 wt % in comparison with neat PLA, but the flexural strength decreases with increasing fiber loading. There is an increasing trend for the flexural strength for all composites after the addition of WFs. Neat PLA has a flexural strength and modulus of 98.8 MPa and 3.3 GPa, respectively, whereas the PLA/WF (60 wt %/40 wt %) composite has a flexural strength and modulus of 114.3 MPa and 10.2 GPa, respectively. The flexural strength increases significantly from 98.8 to 118.3 MPa in the presence of 20 wt % WF, and thereafter the flexural strength decreases to 114.3 MPa, despite the fiber content increasing to 40 wt %. The flexural modulus increases significantly with the addition of WFs. The large increase in the modulus suggests efficient stress transfer between the polymer and fiber.[8,15] Our present studies on WF-reinforced PLA composites indicate that the flexural properties are superior to most types of WF-reinforced thermoplastic composites studied by several other investigators.[1,2,5] These results indicate that the stiffness of these new materials is very high.

Figure 1 illustrates the flexural modulus of the PLA composites with various fiber contents. These results indicate that the flexural modulus increases with the fiber volume fraction and that a linear relationship exists.[8] The fiber volume fraction (v_f) can be calculated with eq. (1):

$$v_f = 100(w_f/\rho_f)/[(w_m/\rho_m) + (w_f/\rho_f)] \quad (1)$$

where w_m is the weight fraction of the matrix in the composite, ρ_m is the density of the matrix, w_f is the weight fraction of the fiber in the composite, and ρ_f is the density of the fiber. The densities of the PLA matrix, PP matrix, and WF are 1.25, 0.91, and 1.4 g/cm^3, respectively.

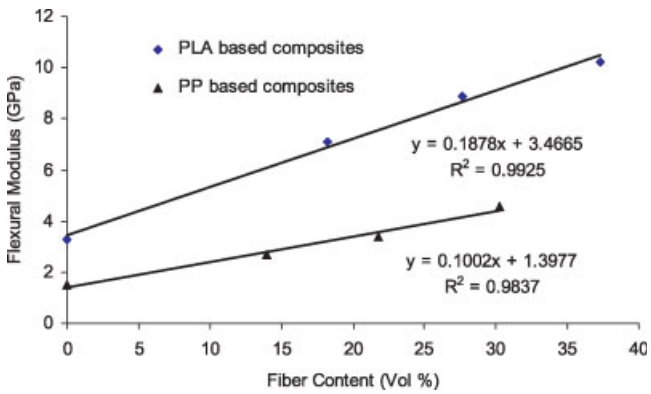

Figure 1 Flexural modulus of the PLA/WF and PP/WF composites. [Color figure can be viewed in the online issue, which is available at www.interscience.wiley.com.]

Table I and Figure 1 also give the mechanical properties of the PP and PP-based composites. Both the flexural modulus and flexural strength of PP increase significantly with the addition of WFs. Figure 1 shows that the PLA-based composites possess higher flexural moduli than the PP-based composites. Table II gives the mechanical properties of the WF-reinforced PLA- and PP-based composites in the presence of MAPP. Compared with those of the neat resin, the flexural properties of both the PLA/MAPP (95/5) and PP/MAPP (95/5) blends are significantly higher. According to Keener et al.,[29] as MAPP polymers chemically link to the surface of the reinforcement/filler, it also co-crystallizes with the base polymer, creating a composite with increased thermal and physical properties. In addition, MAPP polymers enhance the interfacial adhesion between polar substrates and nonpolar polymers. Table II also shows the effect of MAPP on the mechanical properties of the WF composites. The flexural strength of the PLA/WF/MAPP composite decreases with the addition of 5 wt % MAPP in comparison with the PLA/WF (70/30) composite. On the contrary, both the flexural modulus and flexural strength of the PP/WF/MAPP composite increase significantly after the addition of 5 wt % MAPP. Here, because MAPP can interact with hydroxyl groups at the WF surface, MAPP improves the compatibility between PP and WF, and the chain entanglement between PP and MAPP is formed because of the similar molecular chain structure.[21] Kazayawoko et al.[23] stated that MAPP may react with the hydroxyl groups of WFs by esterification, as depicted in Figure 2. The forma-

TABLE II
Flexural Properties of the Composites

Polymer/ fibers (wt %)	Flexural strength (MPa)	Flexural modulus (GPa)	Improvement in the modulus (%)
Neat PLA	98.8 ± 1.0	3.3 ± 0.1	—
PLA/MAPP (95/5)	111.8 ± 0.6	6.1 ± 0.0	84
PLA/WF/MAPP (65/30/5)	75.3 ± 1.8	8.6 ± 0.2	161
Neat PP	32.9 ± 1.8	1.5 ± 0.2	—
PP/MAPP (95/5)	44.0 ± 0.8	2.3 ± 0.0	53
PP/WF/MAPP (65/30/5)	64.6 ± 1.3	3.9 ± 0.4	160

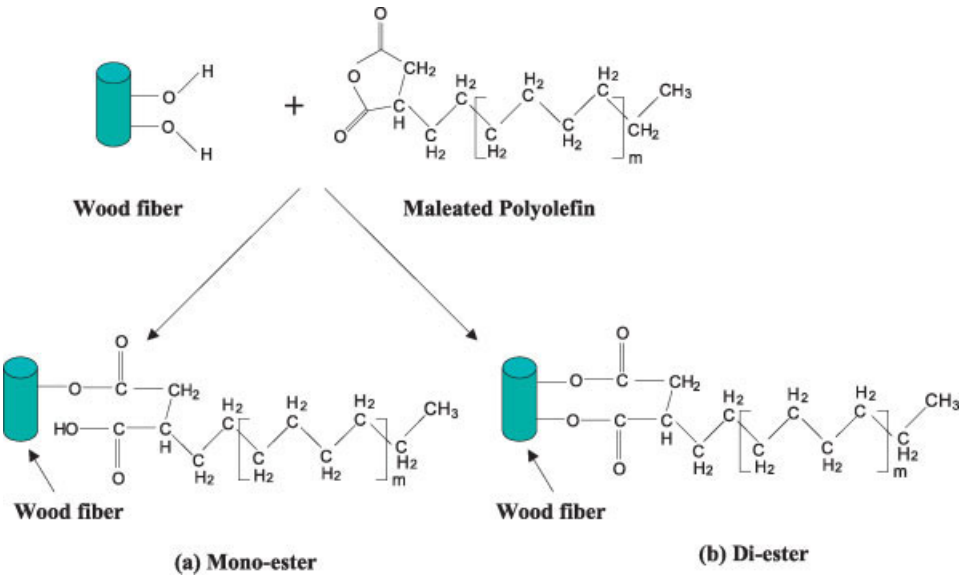

Figure 2 Possible chemical reactions of WFs with MAPP. [Color figure can be viewed in the online issue, which is available at www.interscience.wiley.com.]

tion of covalent linkages between hydroxyl groups of cellulose fiber and MA was described by Hedenberg and Gatenholm[30] through IR and electron spectroscopy for chemical analysis. Moreover, Table II shows that the flexural strength of the PLA composite decreases with the addition of MAPP, and it is probable that the existence of the less than adequate adhesion between the WFs and PLA results in the reduced flexural strength values. Recently, Plackett[31] and Lanzilotta et al.[32] studied the melt modification of PLA with MA. Plackett suggested that the PLA mechanical properties are closely correlated with the molecular weight, and the mechanical testing of PLA/jute composites showed a reduction in the mechanical strength resulting from the addition of maleated PLA to the fibers. Lanzilotta et al. discovered that the mechanical strength of injection-molded PLA was not improved when 20–40 wt % flax was incorporated, and the authors attributed this to poor adhesion between the flax and PLA, which had been modified with MA by reactive extrusion.

Tensile properties of the composites

The tensile properties of the PLA matrix and PLA-based composites are shown in Table III. The tensile modulus increases significantly with the addition of 20 or 30 wt % WF, and the tensile strength remains nearly same. This reveals that the incorporation of WFs into the matrix provides effective reinforcement. The further addition of WFs increases the modulus, but the tensile strength of the 40 wt % WF-reinforced PLA composite decreases in comparison with neat PLA. It is obvious from Table I that there is a significant increase in the flexural strength from a 20 to 40 wt % fiber loading in comparison with neat PLA, but it decreases with the fiber loading. Similarly, in Table III, the tensile strength increases with an increase in the fiber loading up to 30 wt % and thereafter decreases. Usually, the orientation of WFs in composites influences the tensile strength of fiber-reinforced composites.[2,5] The better the fibers are aligned, the higher the strength values can be. English and Falk[2] suggested that this increase in the mechanical strength up to a 30 wt % fiber loading is due to increased wetting of fibers with the matrix resin. On the other hand, the decrease in the mechanical strength upon subsequent loading may be due to inadequate wetting of the fiber with the matrix, which leads to easy composite failure.[5] Park and Balatinecz[3] reported that the ultimate strain decreased as the WF content increased because of the decreased deformability of the matrix, which was restricted by the rigid particles. The effect of the WF content on the tensile properties of WF-reinforced PLA composites is shown in Figure 3. Figure 3 shows both the measured values and theoretical estimations of the prop-

TABLE III
Tensile Properties of the PLA-Based Composites

Polymer/ fibers (wt %)	Tensile strength (MPa)	Tensile modulus (GPa)	Improvement in the modulus (%)
Neat PLA	62.8 ± 4.9	2.7 ± 0.4	—
PLA/WF (80/20)	65.7 ± 1.3	4.8 ± 0.6	77
PLA/WF (70/30)	63.3 ± 5.8	5.3 ± 0.8	96
PLA/WF (60/40)	58.7 ± 3.1	6.3 ± 0.9	133

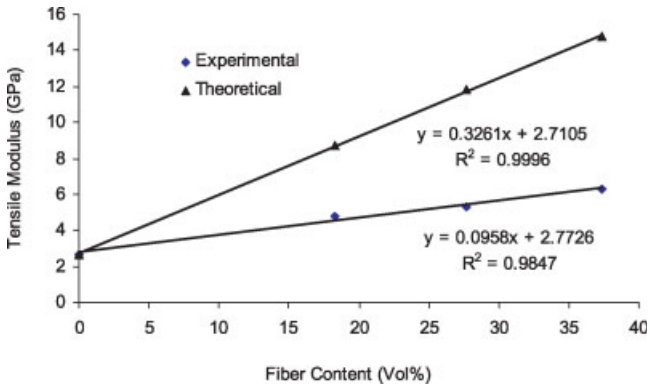

Figure 3 Tensile modulus versus the volume fraction for PLA/WF composites with theoretical estimations. [Color figure can be viewed in the online issue, which is available at www.interscience.wiley.com.]

erties versus the fiber volume fraction. The theoretical estimations can be calculated with the rule of mixture:[6]

$$E_c = E_f v_f + (1 - v_f)E_m \quad (2)$$

where E_c is the tensile modulus of the composite, v_f is the volume fraction of the fiber, E_f is the tensile modulus of the fiber, and E_m is the tensile modulus of the matrix.

WF-reinforced PLA composites follow the rule of mixtures. The tensile modulus depends linearly on the WF content in these composites.[8] The modulus of PLA increases proportionately as the amount of WFs in the composite increases.[8] Usually, the increase in the tensile modulus is consistent with the rule of mixtures, which stipulates reinforcement of the matrix by fibers that are capable of transferring stresses across the fiber–matrix interface. Both theoretical and experimental tensile moduli present the same increasing trend with the increase in the WF content; however, the values of the former are higher than those of the latter. The poor adhesion between the WFs and PLA matrix can be considered the reason that the experimental tensile modulus is lower than the theoretical one. The WFs appear to be randomly oriented to the naked eye; that is, unidirectional orientation along the flow direction has not been observed in injection-molded specimens. Manikandan et al.[33] observed that the random orientation could be attributed to a low flow speed due to the use of a hand-operated, ram-type injection-molding machine. Moreover, because the fiber orientation is random throughout the composite samples and there is no modification on the surface of the fiber being used to make the composites, the variation of the theoretical and experimental modulus values seems reasonable. Additionally, the fibers may not be uniformly distributed throughout the dog-bone-shaped composite specimens during the fabrication process of the composite. In natural-fiber-reinforced composites, weak adhesion may result from poor dispersion and incompatibility between the hydrophilic natural fibers and the hydrophobic polymer.[5]

TABLE IV
Notched Izod Impact Strength of the Composites

Polymer/ fibers (wt %)	Notched Izod impact strength (J/m)	Improvement (%)
Neat PLA	25.7 ± 1.3	—
PLA/WF (80/20)	23.9 ± 0.7	—
PLA/WF (70/30)	23.2 ± 2.9	—
PLA/WF (60/40)	21.9 ± 3.3	—
PLA/MAPP (95/5)	26.5 ± 2.7	3
PLA/WF/MAPP (65/30/5)	24.5 ± 0.6	—
Neat PP	29.7 ± 3.1	—
PP/WF (80/20)	57.6 ± 5.9	93
PP/WF (70/30)	46.4 ± 1.8	56
PP/WF (60/40)	37.8 ± 3.9	27
PP/MAPP (95/5)	25.5 ± 4.4	6
PP/WF/MAPP (65/30/5)	47.3 ± 4.5	59

Notched Izod impact strength of the composites

The notched Izod impact strength results for the tested materials are shown in Table IV. The impact

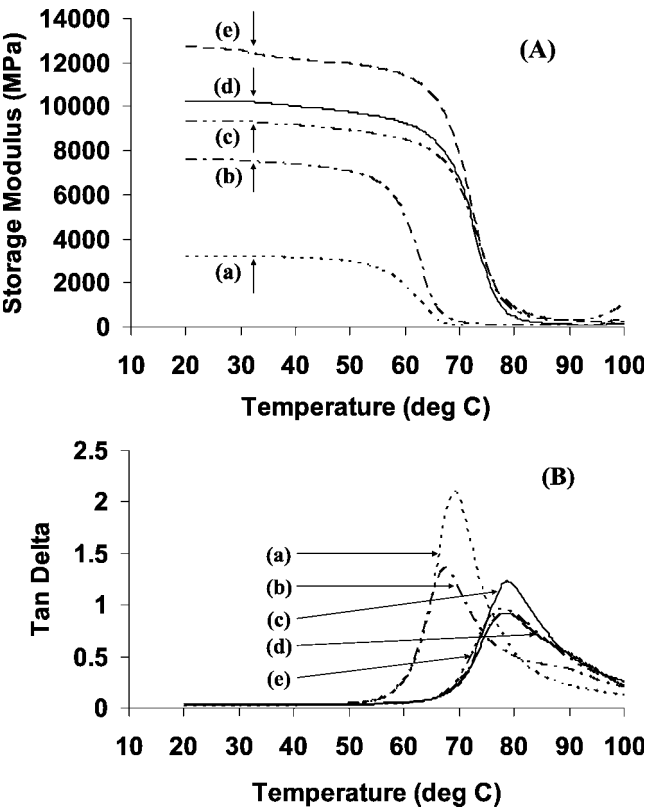

Figure 4 Temperature dependence of (A) the storage modulus and (B) tan δ of PLA and PLA-based composites: (a) neat PLA, (b) PLA/MAPP (95/5), (c) PLA/WF/MAPP (65/30/5), (d) PLA/WF (70/30), and (e) PLA/WF (60/40).

TABLE V
Thermomechanical Properties of the PLA-Based Composites

PLA/fibers (wt %)	T_g (°C)[a]	Storage modulus (GPa) 25°C	40°C	60°C	Reinforcement imparted by the fibers at 25°C to the modulus (%)
Neat PLA	63	3.2	3.1	1.8	—
PLA/WF (80/20)	74	9.3	9.1	8.5	190
PLA/WF (70/30)	77	10.2	10.0	9.2	218
PLA/WF (60/40)	79	12.6	12.1	11.3	293
PLA/WF/MAPP (60/30/5)	78	9.3	9.1	8.4	190
PLA/MAPP (95/5)	62	7.5	7.3	4.8	134

[a] Obtained from the loss modulus curves.

strength of the PLA/WF (60/40) composite changes little after the addition of a higher fiber content in comparison with the PLA/WF (70/30) composite, which has an impact strength of 23.2 J/m. Moreover, the impact strength of both the PLA/WF (70/30) and PLA/WF/MAPP (65/30/5) composites remains about the same even after the addition of 5 wt % MAPP. According to Luo and Netravali,[10] two factors need to be considered to develop sufficient stress-transfer properties between the matrix and the fiber. First, the MAPP present near the fiber surface should be strongly interacting with the fiber surface through covalent bonding. This means that sufficient MA groups should be present in MAPP so that interactions can occur with the hydroxyl groups on the fiber surface. Second, the polymer chains of MAPP should be long enough to permit entanglements with the polymer in the interphase.

Table IV also shows that after the addition of 20 wt % WF, the impact strength of the PP composite improves significantly. The impact strength of the PP/WF (60/40) composite decreases after the addition of a higher fiber content in comparison with the PP/WF (70/30) composite, which has an impact strength of 46.4 J/m. Amash and Zugenmaier[34] reported that the cellulose fibers act as efficient nucleating agents for the crystallization of PP and consequently increase the crystallization rate of PP. Usually, good filler/matrix interfacial adhesion provides an effective resistance to crack propagation during impact tests. In Table IV, even after the addition of 5% MAPP, the impact strength of the PP/WF/MAPP (65/30/5) composite remains nearly the same in comparison with PP/WF (70/30). This finding is in accordance with the results of Rowell et al.[35] The predominant mechanism of energy absorption is crack propagation in the notched Izod test. During crack propagation, the addition of MAPP has little effect on the amount of energy absorbed.[30] Cracks are initiated at points of high stress concentrations such as fiber ends, defects, or the interface region, where the adhesion between the two phases is very poor. Generally, the toughness of short-fiber-reinforced composites can be influenced by a number of factors, such as the intrinsic matrix properties, fiber volume fraction, and interfacial bond strength.[5] Therefore, strong interactions between the anhydride groups of the maleated coupling agent and the hydroxyl groups of natural fibers are needed to overcome the incompatibility problem to increase the impact, tensile, and flexural strengths of WF-reinforced composites.[5,21,23]

Thermomechanical properties

Dynamic mechanical properties of the composites

Figure 4 shows the dynamic storage modulus and tan δ values of the PLA-based composites as a func-

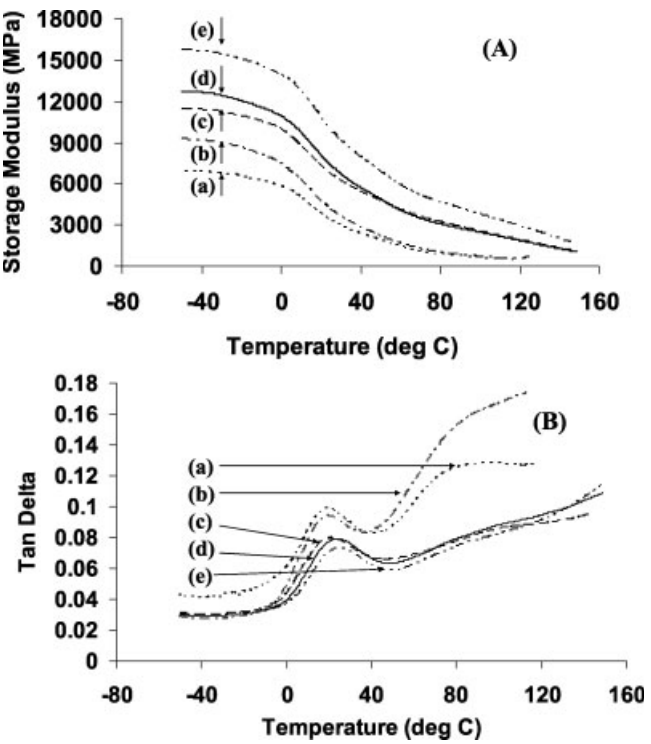

Figure 5 Temperature dependence of (A) the storage modulus and (B) tan δ of PP and PP-based composites: (a) neat PP, (b) PP/MAPP (95/5), (c) PP/WF/MAPP (65/30/5), (d) PP/WF (70/30), and (e) PP/WF (60/40).

TABLE VI
Thermomechanical Properties of the PP-Based Composites

Polymer/fibers (wt %)	Storage modulus (GPa) 25°C	40°C	60°C	Reinforcement imparted by the fibers at 25°C to the modulus (%)
Neat PP	3.3	3.1	1.8	—
PP/WF (80/20)	5.6	4.4	3.1	69
PP/WF (70/30)	7.3	5.7	4.0	121
PP/WF (60/40)	9.8	7.9	5.8	196
PP/WF/MAPP (65/30/5)	6.6	5.3	4.0	100
PP/MAPP (95/5)	4.0	2.8	1.6	21

tion of temperature. As shown in Figure 4(A) and Table V, the storage modulus of the PLA-based composites is higher than that of the PLA matrix. This is due to the reinforcement imparted by the WFs, which allows effective stress transfer from the matrix to the WFs.[15] We have found that the storage moduli increase with the incorporation of WFs into PLA. Although loss modulus curves have been omitted for the sake of brevity, the T_g values, derived from the loss modulus curves, are included in Table V. T_g is usually interpreted as the peak of the loss modulus curves obtained during a dynamic mechanical test.[36] As shown in Table V, T_g of the PLA-based composites shifts to higher temperature because of the fiber present in the PLA matrix. The shifting of T_g to higher temperatures can be associated with the decreased mobility of the matrix chains due to the addition of fibers. Moreover, as shown in Figure 4(A), the neat PLA shows a sharp drop in the storage modulus near the T_g region. Above 65°C, which is higher than the T_g region of neat PLA, the storage modulus of the PLA-based composites shows a sudden drop because the glassy, amorphous molecules turn into a rubbery phase.[36,37] As the WF content increases in the composites, the storage modulus drop gradually shifts to a higher temperature. The abrupt increase in the storage modulus drop above 65°C shown for the PLA-based composites reflects an increase in the rigidity of the composite material due to the presence of WFs. This observation indicates that the rigidity of the composite material increases as the WF content increases. In the case of the PLA/MAPP blend, T_g of PLA/MAPP remains nearly the same in comparison with T_g of neat PLA.

According to the tan δ curves [Fig. 4(B)], a remarkable move of the tan δ peak toward a higher temperature can be achieved in the presence of WFs. The tan δ peak is shifted to a higher temperature with the WF content. A shift to a higher temperature usually indicates restricted molecule movement because of improved interaction in filled PLA polymers.[6,37] In addition, the tan δ peak height is reduced with increasing proportions of WFs. As shown in Figure 4(B), the incorporation of fibers reduces the tan δ peak height by restricting the movement of the PLA polymer molecules.

Generally, tan δ is the ratio of the storage modulus to the loss modulus, which is a measure of the energy loss in relation to the recoverable energy.[36] Nielsen and Landel[38] suggested that the damping in the transition region measures the imperfection in the elasticity and that much of the energy used to deform a material during DMA testing is dissipated directly into heat. Hence, the molecular mobility of the composites decreases and the mechanical loss to overcome interfriction between molecular chains is reduced after the addition of fibers. The addition of

TABLE VII
HDT of the Composites

Polymer/fibers (wt %)	HDT (°C)
Neat PLA	64.5
PLA/WF (70/30)	66.1
PLA/WF (60/40)	67.6
PLA/MAPP (95/5)	64.2
PLA/WF/MAPP (65/30/5)	69.0
Neat PP	106.3
PP/WF (70/30)	139.4
PP/WF (60/40)	151.1
PP/MAPP (95/5)	91.9
PP/WF/MAPP (65/30/5)	153.7

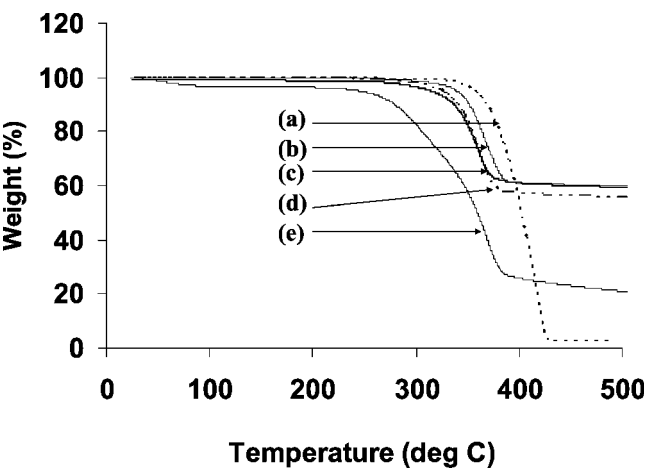

Figure 6 Thermogravimetric curves of PLA, WFs, and composites: (a) neat PLA, (b) PLA/WF (80/20), (c) PLA/WF (70/30), (d) PLA/WF (60/40), and (e) neat WFs.

TABLE VIII
TGA Characterization of the Composites

Polymer/fibers (wt %)	T_5 (°C)	T_{25} (°C)	T_{50} (°C)	T_{75} (°C)
Neat PLA	356	385	401	414
PLA/WF (80/20)	337	368	> 500	> 500
PLA/WF (70/30)	324	358	> 500	> 500
PLA/WF (60/40)	319	352	> 500	> 500
Neat PP	393	441	456	465
PP/WF (70/30)	313	427	458	471
PP/WF (60/40)	297	376	454	471
WF	245	317	359	413

5% MAPP also reduces the storage modulus of PLA/WF/MAPP composite. The presence of MAPP could reduce the transition temperature by enhancing the ability of the polymer to undergo a glass–rubber transition, and the molecular mobility associated with this transition is complicated.[38,39] The presence of WFs adds to the complexity. With respect to the lower stiffness values of the maleic acid anhydride grafted composite material, Sanadi et al.[40] stated that this effect can be explained by two phenomena: the formation of a stiffer polymer phase around the fibers in the system without a coupling agent or an altered fiber orientation caused by the addition of a coupling agent.

Figure 5 shows the dynamic storage modulus and tan δ of the PP-based composites as functions of temperature. As shown in Figure 5(A) and Table VI, the moduli increase in the presence of WFs in the composites. The storage modulus of PP-based composites is higher than that of the PP matrix; and this indicates that stress transfers from the matrix to the WF. Figure 5(B) shows that the tan δ values of the PP/WF composite are lower than those for the PP matrix at low temperatures. The tan δ values for the composite increase with increasing temperature. The incorporation of fibers reduces the tan δ peak height by restricting the movement of the PP polymer molecules [Fig. 5(B)]. We have found that the storage moduli increase significantly with the incorporation of WF into PP when no coupling agent is added. As shown in Table VI, even at high temperatures, the storage moduli remain significantly high for the reinforcement imparted by the WFs. As shown in Figure 5(B), the addition of 5 wt % MAPP does not increase the storage modulus of the PP/WF/MAPP (65/30/5) composite in comparison with the PP/WF (70/30) composites. Usually, a coupling agent is capable of reacting with the functional groups at the surface of the fiber or filler, whereas the backbone of the polymer is miscible with the base PP. Arencón et al.[41] suggested that MAPP addition to both PP and a PP/copoly(ethylene terephthalate-*co*-isophthalate) (95/5) blend did not modify the PP crystallization characteristics. Some investigators[42–44] have observed that small amounts of MAPP act as nucleating agents in homopolymer PP, although Arencón et al. did not observe this effect.

Heat deflection temperature (HDT) of the composites

One of the most striking effects of WFs in composites is the great increase in HDT. The HDT of the WF-reinforced PLA composites is higher than the HDT of the PLA resin, and this value suggests the upper service temperature limit for a plastic. HDT is a short-term thermal property that measures the thermal sensitivity and stability of resins. Table VII reveals that the HDT of the composites increases with the WF content. As the WF content approaches 30–40 wt %, the HDT of the composite increases from 66.1 to 67.6°C for PLA-based composites and from 139.4 to 151.1°C for PP-based composites. This might be due to better reinforcement of the fiber.

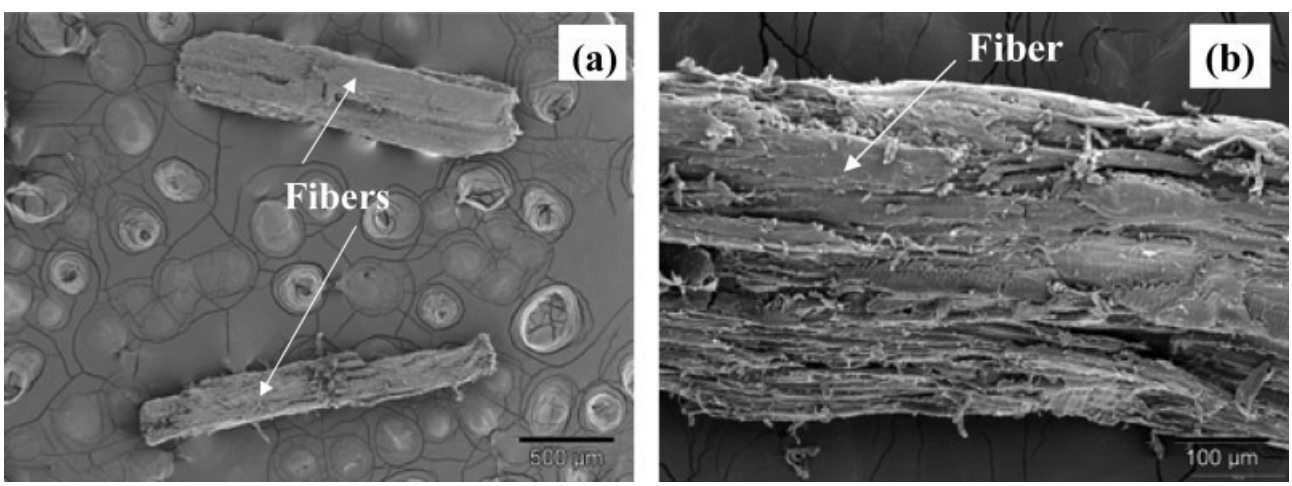

Figure 7 SEM micrographs of WFs: (a) 500 and (b) 100 µm.

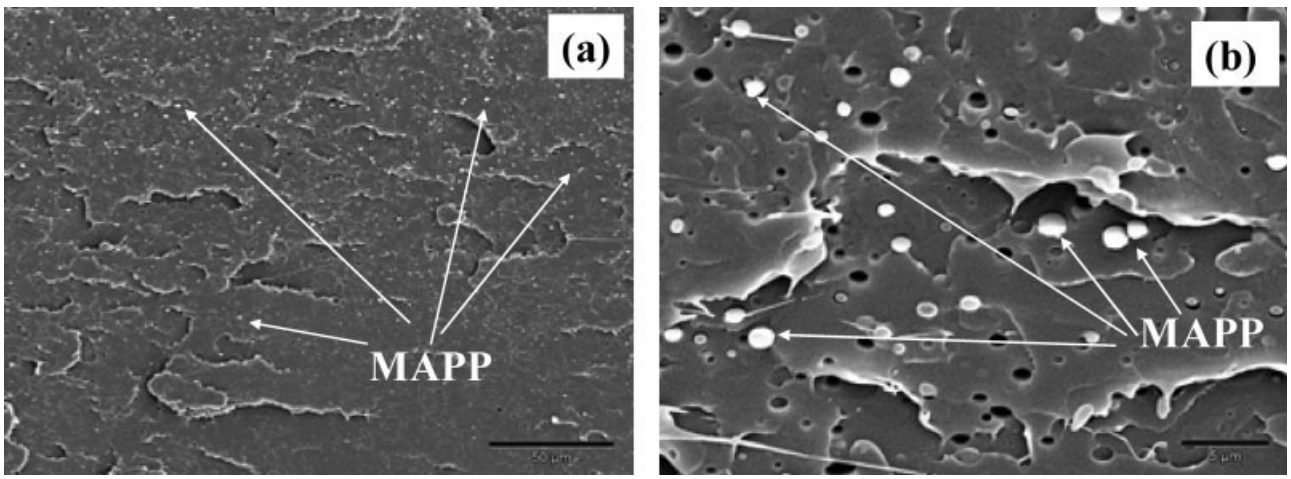

Figure 8 SEM micrographs of the PLA/MAPP (95/5) composite: (a) 50 and (b) 5 μm.

Table VII shows that the HDT of the PLA/MAPP (95/5) blend is 64.2. On the contrary, the WF-reinforced composite with 5 wt % MAPP exhibits a high HDT; for example, the HDT of the PLA/WF composite with 5% MAPP is 69°C. The HDT of the WF-reinforced PP composites is higher than that of the PP resin. Even without reinforcement, the HDT of PP exceeds 106°C. Table VII also shows that the HDT of PP/WF (60/40) is relatively high compared with that of the PP/WF (70/30) composite. This means a higher service temperature capability in general. The HDT of PP/MAPP (95/5) is lower than the HDT of neat PP. Because better chemical bonding exists between the PP matrix and WF, the composite with 5 wt % MAPP exhibits a higher HDT than the PP/WF (70/30) composite; for example, the HDT of the PP/WF/MAPP (65/30/5) composite is 153.7°C (an increase of 10%). In general, increasing the crystallinity and reinforcement are the main options to increase the HDT of a polymer. In this context, the increase in the HDT of neat PP by reinforcement with WFs is an important finding.

Thermogravimetry

The TGA curves of PLA, WF, and PLA-based composites are presented in Figure 6. The TGA curve of neat WF shows a 5% weight loss peak at 245°C, followed by another 74% weight loss peak at 389°C. In general, there are three stages of degradation throughout the temperature runs, especially for WF. This is consistent with the results reported by Van de Velde and Baetens.[45] As shown in Figure 6, the initial weight loss of WFs occurs approximately until 238°C because of the heat of evaporation of moisture in the WF and the initial decomposition of cellulose and hemicellulose. The severe weight loss from 238 to 389°C is due to the major components of WFs, namely, cellulose, hemicellulose, and lignin. At a temperature of 389°C, the maximum percentage of

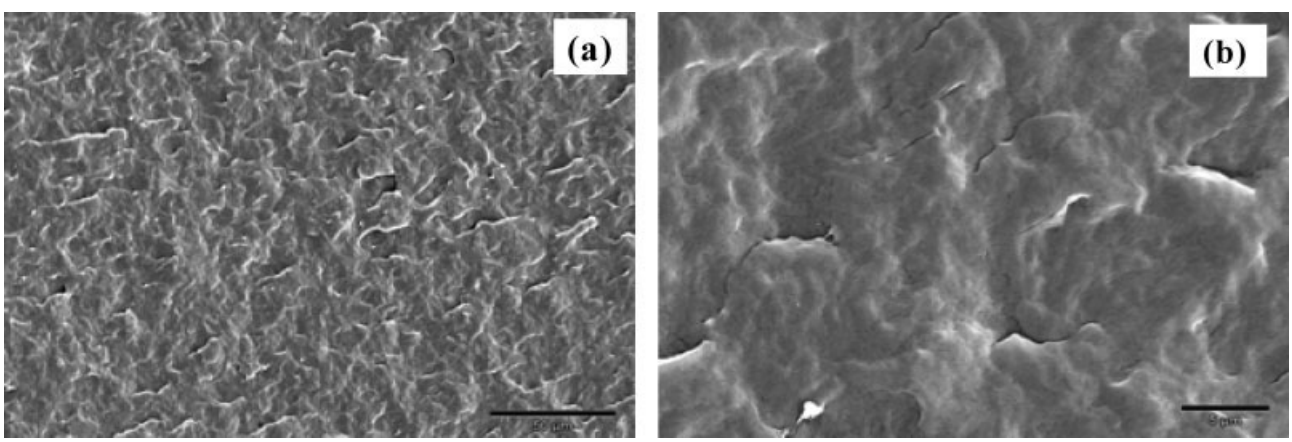

Figure 9 SEM micrographs of the PP/MAPP (95/5) composite: (a) 50 and (b) 5 μm.

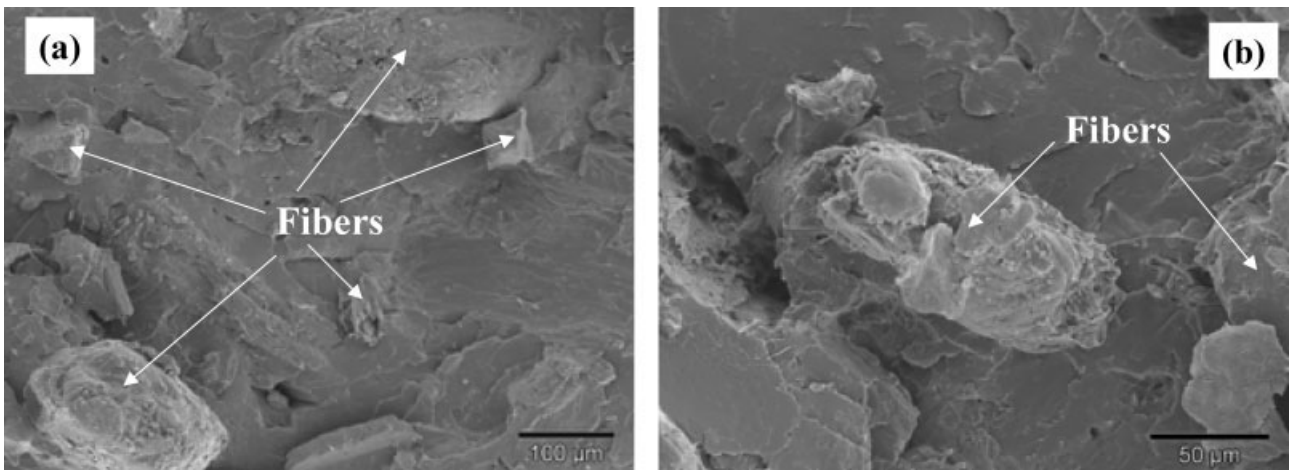

Figure 10 SEM micrographs of the PLA/WF (70/30) composite: (a) 100 and (b) 50 μm.

cellulose and hemicellulose decomposes. According to Shafizadeh and DeGroote,[46] the cellulose and hemicellulose components of WFs are the major contributors to decomposition between 200 and 400°C, whereas lignin is mainly responsible for the char formation of WFs over 400°C. The decomposition of neat PLA starts at 319°C, and nearly 98.6% of the decomposition occurs at 433°C. This decomposition temperature range of neat PLA is higher than that of neat WFs.

The thermal stability of PLA- and PP-based composites has also been investigated with TGA. In Table VIII, for all specimens, the 5, 25, 50, and 75% weight loss temperatures (T_5, T_{25}, T_{50}, and T_{75}, respectively) are listed, and they were derived from plots of the weight (%) versus the temperature for each sample. At 350°C, there are 8, 11, and 17% weight losses for the PLA/WF (80/20), PLA/WF (70/30), and PLA/WF (60/40) composites, respectively. As the WF content increases, the thermal stability of the composites decreases. This result indicates that the compatibility and interfacial bonding decreases by the mixing of both the PLA polymer and WFs. Moreover, there are 90 and 92% weight losses at 500°C for the PP/WF (60/40) and PP/WF (70/30) composites, respectively. The thermal stability of the composite is in the order of PP/WF (60/40) < PP/WF (70/30), which indicates that the thermal stability of the composites decreases as the WF content increases. Similar results have been reported by Wielage et al.[47] for natural-fiber-reinforced PP composites. The TGA data in Table VIII reveal that the thermal stability of the PLA composites containing WF may be as good as that of PP reinforced with WF.

Morphology of the composites

SEM micrographs exhibit fibers of different diameters ranging from 330 to 410 μm (Fig. 7). The average length of the fibers is about 1650 μm. Figure 8 shows that nonactivated MAPP remains at the interface for

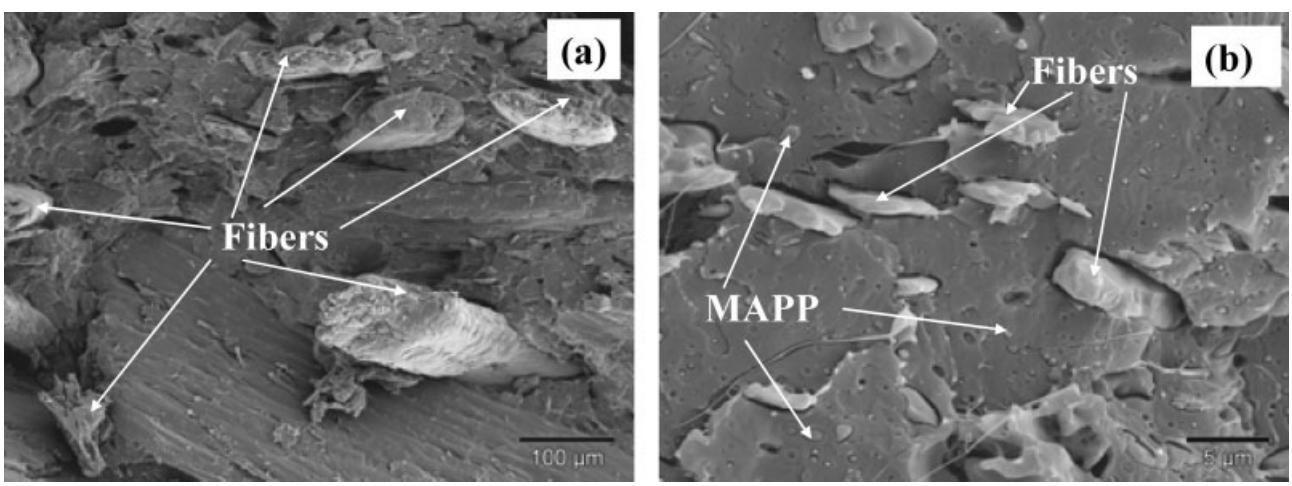

Figure 11 SEM micrographs of the PLA/WF/MAPP (65/30/5) composite: (a) 100 and (b) 5 μm.

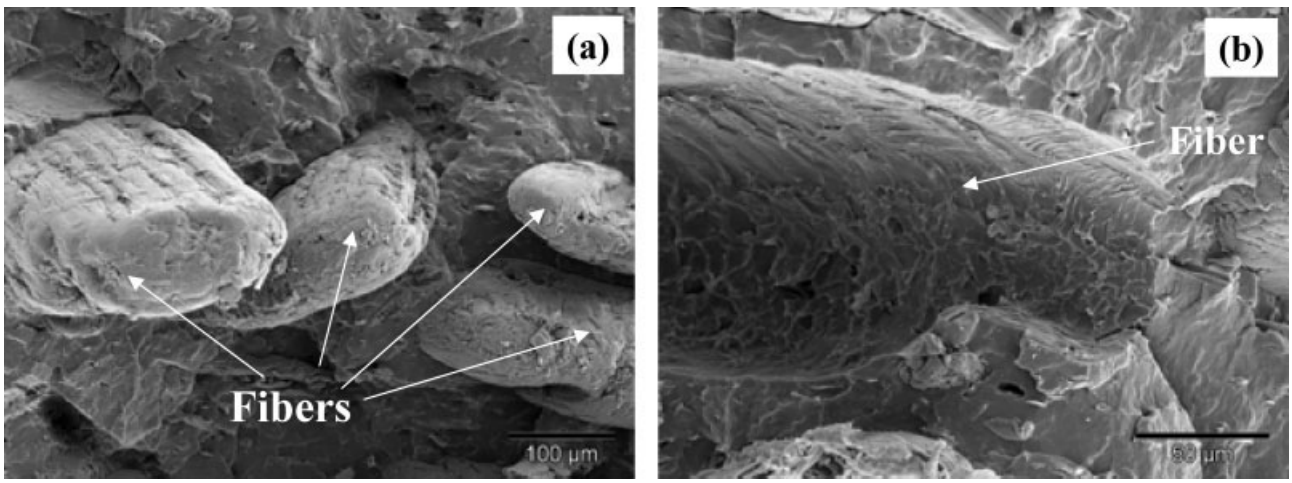

Figure 12 SEM micrographs of the PP/WF (70/30) composite: (a) 100 and (b) 50 μm.

the PLA/MAPP (95/5) blend; the size of the MAPP particle is nearly 1 μm or less. Oksman et al.[25] also observed by FTIR spectroscopy that MA is partially bonded to the wood through esterification but that some nonactivated MA remains at the interface. Figure 9 shows SEM micrographs of the fractured surface of a notched Izod impact specimen of the PP/MAPP (95/5) blend, and there is an absence of nonactivated MAPP particles in these micrographs. In Figure 10, SEM micrographs illustrate the individual separation and dispersion of the WFs in the form of single fibers, and this indicates that the WFs have been separated during the extrusion process and are well dispersed in the PLA matrix. In Figure 10(b), the micrograph shows that the matrix is an indication of good fiber–matrix adhesion at a higher magnification.

Here it is difficult to differentiate the WFs from the PLA matrix, and this may suggest that the WFs are coated, probably by the matrix, and that failure most commonly occurs in the matrix and not at the fiber surfaces.[5,21] This also suggests that there is some kind of interfacial contact between the PLA matrix and WFs. In Figure 11, the presence of nonactivated MAPP at the interface can be observed in the PLA/WF/MAPP composite, similarly to Oksman et al.'s study.[25] In our investigation, no differences in the WF dispersion with the addition of MAPP in the PLA matrix have been observed, and voids around the WF surfaces are present, indicating poor adhesion between the WFs and PLA in the presence of MAPP.

Figure 12 presents SEM pictures of the PP/WF composite at magnifications of 100 and 50 μm, whereas Figure 13 presents SEM pictures of the PP/WF/MAPP composite at the same magnifications. The gaps between the fiber and matrix in Figures 12 and 13 can be clearly observed. This gap is very wide in the case of the PP/WF (70/30) composite (Fig. 12), whereas the gaps are narrow in the case of the PP/WF/MAPP (65/30/5) composite (Fig. 13). In Figure 13, if we look closely at the MAPP-treated

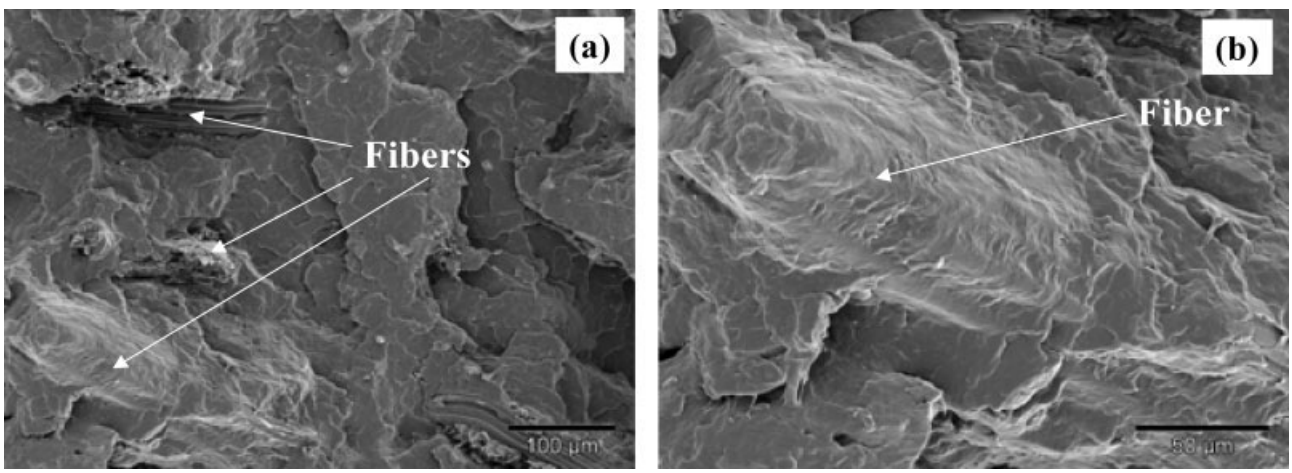

Figure 13 SEM micrographs of the PP/WF/MAPP (65/30/5) composite: (a) 100 and (b) 50 μm.

fiber surface at a higher magnification, we can see that MAPP forms an interphase around the WFs, suggesting good compatibility of the fibers and PP matrix. The fiber pullouts are larger in Figure 12 than those in Figure 13, and this confirms that the interfacial adhesion between the matrix and the fiber is greater in the PP/WF/MAPP composite. Hence, the presence of MAPP has a large positive effect on the mechanical properties of WF-reinforced PP composites in comparison with composites made without MAPP.

CONCLUSIONS

This study demonstrates that WF can be successfully used as a reinforcing fiber material in a biodegradable polymer such as PLA. WF-reinforced PLA- and PP-based composites were prepared with a microcompounding molding system, and their mechanical and thermomechanical properties were investigated. The mechanical and thermomechanical properties of the WF-reinforced PLA composites compared favorably with the corresponding properties of the PP composites. Compared with those of the neat resin, the flexural properties of the PLA composites were significantly higher as a result of reinforcement by WF. On the whole, the flexural properties of all the fiber-reinforced composites increased with the fiber content. An improvement in the flexural properties was possible by WF reinforcement, regardless of the kind of matrix polymer used in this study. According to the DMA results, the incorporation of WFs gave rise to a considerable increase in the storage modulus and a decrease in the tan δ values. These results demonstrated the reinforcing effect of WFs on both PLA and PP matrices. The morphology evaluated by SEM indicated that there were less voids on the fracture surface, and this indicated that the WFs were well trapped by the PLA matrix as well as the PP matrix. The MAPP coupling agent favored a better PP–WF interaction. WFs more effectively served as reinforcements instead of fillers with MAPP. In the case of neat WFs, TGA results showed severe weight loss from 220 to 385°C. For virgin PLA, decomposition started at 345°C, and the process was completed at 430°C. The thermal behavior of the composites was also evaluated with TGA. For the 20 wt % WF-reinforced composite, the degradation began at 328°C, and 50% decomposition occurred at the higher temperature of 500°C. The thermal stability of the composites decreased with the increase in the WF content in the composites. The heat deflection temperature of the composites increased with increasing WF content. Overall, the advantages of using a biodegradable polymer such as PLA as a matrix have been proved because the environmentally friendly composites prepared with this material present good thermal and mechanical properties. Furthermore, the use of WFs as reinforcements in PLA provides interesting alternatives for the production of low-cost and ecologically friendly composites.

The authors express their appreciation to American Wood Fibers (Schofield, WI), Eastman Chemical Co. (Kingsport, TN), Basell Polyolefins (Elkton, MD), and Biomer (Germany) for supplying the wood fiber, Epolene G-3015 polymer, polypropylene, and poly(lactic acid), respectively.

References

1. Wolcott, M. P. Wood Fiber/Polymer Composites—Fundamental Concepts, Processes and Material Options; Forest Products Society: Madison, WI, 1993; p 134.
2. English, B. W.; Falk, R. H. Factors That Affect the Application of Wood Fiber–Plastic Composites; Forest Products Society: Madison, WI, 1995; p 189.
3. Park, B. D.; Balatinecz, J. J. Polym Compos 1997, 18, 79.
4. Bowis, M. E.; Bhattacharyya, D.; Uprichard, M. V. In Progress in Advanced Materials and Mechanics; Tzuchiang, W.; Chou, T. W., Eds.; Peking University Press: Beijing, 1996; p 956.
5. Kazayawoko, M.; Balatinecz, J. J. Adhesion Mechanisms in Wood Fiber–Polypropylene Composites; Forest Products Society: Madison, WI, 1995; p 81.
6. Guo, W.; Ashida, M. J Appl Polym Sci 1993, 50, 1435.
7. Mohanty, A. K.; Misra, M.; Hinrichsen, G. Macromol Mater Eng 2000, 276, 1.
8. Gassan, J.; Bledzki, A. K. Prog Polym Sci 1999, 24, 221.
9. Shibata, M.; Ozawa, K.; Teramoto, N.; Yosomiya, R.; Takeishi, H. Macromol Mater Eng 2003, 288, 35.
10. Luo, S.; Netravali, A. N. Polym Compos 1999, 20, 367.
11. Shibata, M.; Makino, R.; Yosomiya, R.; Takeishi, H. Polym Compos 2001, 9, 333.
12. Vink, E. T. H.; Rabago, K. R.; Glassner, D. A.; Gruber, P. R. Polym Degrad Stab 2003, 80, 403.
13. O'Brien, M.; Gray, J. Federal Trade Commission Announces New Fiber Generic: Cargill Dow's Natureworks™ Fibers Receive First Designation of the Century (accessed March 2002). http://cargilldow.com/release.asp?id-92
14. Verespej, M. Winning Technologies: Polylactic Polymers. Ind Week 2000 December 11, p 97.
15. Huda, M. S.; Mohanty, A. K.; Misra, M.; Drzal, L. T.; Schut, E. J Mater Sci 2005, 40, 4221.
16. Oksman, K.; Skrifvars, M.; Selin, J. F. Compos Sci Technol 2003, 63, 1317.
17. Kasuga, T.; Ota, Y.; Nogami, M.; Abe, Y. Biomaterials 2001, 22, 19.
18. Mohanty, A. K.; Misra, M.; Drzal, L. T. J Polym Environ 2002, 10, 19.
19. Stark, M. N.; Rowlands, R. E.; Wood Fiber Sci 2003, 35(2), 167.
20. Carlson, D.; Nie, L.; Narayan, R.; Dubois, P. J Appl Polym Sci 1999, 72, 477.
21. Kazayawoko, M.; Balatinecz, J. J.; Matuana, L. M. J Mater Sci 1999, 34, 6189.
22. Matias, M.; De La Orden, M. U.; Gonzalez Sanchez, C.; Martinez Urreaga, J. J Appl Polym Sci 2000, 75, 256.
23. Kazayawoko, M.; Balatinecz, J. J.; Woodhams, R. T. J Appl Polym Sci 1997, 66, 1163.
24. Gatenholm, P.; Felix, J.; Klason, C.; Kubat, J. In Cellulose–Polymer Composites with Improved Properties; Salamone, J. C.; Riffle, J., Eds.; Contemporary Topics in Polymer Science 7; Plenum: New York, 1992.

25. Oksman, K.; Lindberg, H.; Holmgren, A. J Appl Polym Sci 1998, 69, 201.
26. Lee, S. H.; Ohkita, T.; Kitagawa, K.; Kimura, A. Polym Prepr Jpn 2003, 52, 4308.
27. Lee, S. H.; Ohkita, T. J Appl Polym Sci 2003, 90, 1900.
28. Huda, M. S.; Drzal, L. T.; Misra, M.; Mohanty, A. K.; Williams, K.; Mielewski, D. F. J Ind Eng Chem Res 2005, 44, 5593.
29. Keener, T. J.; Sturat, R. K.; Brown, T. K. Compos A 2004, 35, 367.
30. Hedenberg, P.; Gatenholm, P. J Appl Polym Sci 1995, 56, 641.
31. Plackett, D. J Polym Environ 2004, 12, 131.
32. Lanzilotta, C.; Pipino, A.; Lips, D. Proc Annu Tech Conf Soc Plast Eng 2002, 60, 2185.
33. Manikandan, K. C.; Diwan, S. M.; Thomas, S. J Appl Polym Sci 1996, 60, 1483.
34. Amash, A.; Zugenmaier, P. Polym Bull 1998, 40, 251.
35. Rowell, R. M.; Lange, S. E.; Jacobson, R. E. Mol Cryst Liq Cryst 2000, 353, 85.
36. Menard, K. P. Dynamic Mechanical Analysis: A Practical Introduction; CRC: New York, 1999.
37. Rana, A. K.; Mitra, B. C.; Banerjee, A. N. J Appl Polym Sci 1999, 71, 531.
38. Nielsen, L. E.; Landel, R. F. Text Res J 1994, 64, 696.
39. Järvelä, P.; Shucai, L.; Järvelä, P. J Appl Polym Sci 1996, 62, 813.
40. Sanadi, A. R.; Cauldfield, D. F.; Rowell, R. M. Plast Eng 1994, 4, 27.
41. Arencón, J. I.; Velasco, M. A.; de Saja Rodríguez-Pérez, J. A. J Appl Polym Sci 2004, 94, 1841.
42. Seo, Y.; Kim, J.; Kim, K. U.; Kim, Y. C. Polymer 2000, 41, 2639.
43. Cho, K.; Li, F.; Choi, J. Polymer 1999, 40, 1719.
44. Duvall, J.; Sellitti, C.; Myers, C.; Hiltner, A.; Baer, E. J. J Appl Polym Sci 1994, 52, 207.
45. Van de Velde, K.; Baetens, E. Macromol Mater Eng 2001, 286, 342.
46. Shafizadeh, F.; DeGroote, W. F. In Thermal Uses and Properties of Carbohydrates and Lignins; Shafizadeh, F.; Sarkanen, K. V.; Tillman, D. A., Eds.; Academic: New York, 1976; p 1.
47. Wielage, B.; Lampke, T.; Mark, G.; Nestler, K.; Starke, D. Thermochim Acta 1999, 337, 169.